Korean J. of Chem. Eng., 9(3), 150-158 (1992)

SECONDARY FLOW INDUCED BY INERTIA IN A THIN-FLUID LAYER BETWEEN TWO PARALLEL PLATES

Jeong Jin Hong, Jae Hun Chun and Seung-Man Yang*

Department of Chemical Engineering, Korea Advanced Institute of Science and Technology, 373-1 Kusung-dong, Yusung-ku, Taejon 305-701, Korea

(Received 11 March 1992 • accepted 22 May 1992)

Abstract—The present paper is concerned with the motion of fluid layer between two parallel concentric circular plates, when the inertia of fluid is not negligible. We consider the two specific problems to examine the inertia effects; one in which an incompressible Newtonian fluid is injected into the gap through the hole located at the center of each plate and the other in which two parallel plates rotate coaxially with arbitrary angular velocities. The method of solution is an asymptotic expansion which is usually employed for the thin-film lubrication problem in the limit of small but finite Reynolds number based on the gap height. The asymptotic solutions for the two problems considered here provide the inertia-induced secondary flow patterns, which in turn determine the inertia contributions to the flow parameters such as the pressure drop, injection flow rate, and torque required to sustain the rotation of each plate.

INTRODUCTION

In this paper, we consider the motion of thin fluid layer between two parallel plane surfaces for the thin-film lubrication limit in which the gap height between the plates is small compared to their dimension in the flow direction. In particular, we examine the two specific problems; one in which an incompressible Newtonian fluid is injected to the gap between two concentric disks through the hole located at the center of each disk and the other in which the thin-fluid layer is set in motion owing to the rotating disks (see Figures 1 and 2). The radial flow between the two parallel disks, which is driven by the pressure drop along the gap can be modeled as a radial source flow [1]. This type of flow is of practical significance in the field of polymer processing such as plastic molding and relevant to some aspects of the centrifugal compressor diffusers and the hydrostatic air bearing. The configuration of flow between rotating disks arises in many applications, including lubrication and polymer processing, and it is also relevant to rheometry design for measurement of rheological properties.

Although the flow configuration considered here is simple, it is not possible to solve exactly (except by numerical method) when the inertia of intervening fluid is not negligible. Raal [1] obtained numerical result for radial source flow between parallel disks from a finite-difference solution of the full Navier-Stokes equation with a discretization procedure based on the method of Allen and Southwell [2]. As pointed out by Bird, Stewart and Lightfoot [3], without inertia the velocity profile in the gap is radial and parabolic and the average radial velocity decreases radially as r^{-1}. When the fluid inertia is not negligible, however, Raal showed that the inertia of the intervening fluid creates separation and reverse flow with reattachment further downstream. The problem for steady motion of a viscous fluid confined between two coaxial disks can be reduced to the solution of a coupled set of ordinary differential equations using a similarity transformation developed by von Karman [4]. This solution is also not yet given analytically owing to the nonlinear terms arising from fluid inertia [5].

The vast majority of existing analytical solutions have been for thin-fluid layer where the Reynolds number based on the gap height is sufficiently small for all inertia effects to be neglected, the so-called lubrication limit [6-8]. However, even in the lubrication limit (*i.e.*, small but finite Reynolds number limit, $0 < Re \ll 1$) the inertia of fluid was shown to produce a weak secondary motion which has a velocity component perpendicular to the disks. The inertia-induced secondary flow leads to change in flow characteristics.

*To whom all correspondence should be addressed.

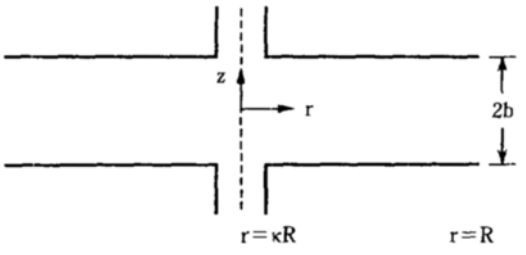

Fig. 1. Schematic description for the radial source flow between two parallel disks.

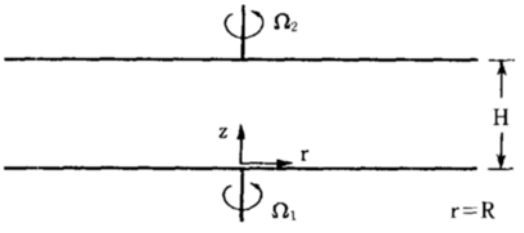

Fig. 2. Schematic description for the flow between two coaxially rotating disks.

For example, the linear relationship between the pressure drop and the injection flow rate in the radial source flow [3] is no longer valid due to the inertia contribution at small but nonzero Reynolds number. For the flow between rotating disks, the torque required to sustain the rotational motion is a linear function of the angular velocity in the absence of fluid inertia [5]. As we shall see shortly, the inertia or centrifugal force generates a weak secondary flow which in turn yields a nonlinear contribution to the torque at $O(Re^2)$. In the present paper, we present an asymptotic result in the limit of small but finite Reynolds number based on the gap height, which is typical of lubrication-theory analysis [9-11]. In section 2, the radial source flow between two parallel coaxial disks is considered for the two different cases; first, we determine the inertia contribution to the injection rate with the pressure drop fixed at a constant value and, in the other case, we examine the inlet-pressure variation induced by inertia with a fixed injection rate. Finally, in section 3, we consider the flow due to coaxially rotating disks with arbitrary angular velocities. The purpose of this section is to show that there are one-parameter families of solutions in the limit of small Reynolds number. The unique parameter classifying the solution families is shown to be the ratio of the angular velocities of the two coaxial disks. In addition, we also present the nonlinear relationship between the hydrodynamic torque on each disk and its angular velocity from the inertia corrections to the lubrication approximation.

RADIAL SOURCE FLOW BETWEEN PARALLEL DISKS

1. Formulation of the Problem

The present problem is concerned with the inertia effects in the steady radial source flow between two parallel disks. An incompressible Newtonian fluid with a constant viscosity μ and a density ρ is injected to the hole of radius a at the center of each disk and then flows radially along the gap between the parallel disks with radius R. The separation distance $2b$ and the radius of the inlet hole a are assumed to be very small compared to the disk radius R.

$$\varepsilon \equiv \frac{b}{R} \ll 1 \text{ and } \kappa \equiv \frac{a}{R} < 1 \tag{1}$$

To solve this problem, we consider the velocity distribution $\vec{u}=(u, v, w)$ in the cylindrical coordinates (r, θ, z). A schematic of the coordinate system is shown in Figure 1. Due to the axisymmetry of the geometry of the thin-film region, the velocity field generated in the gap will be axisymmetric, *i.e.*, $v=0$ and $\partial/\partial\theta=0$ everywhere. The coordinates may be considered to be nondimensionalized with respect to the characteristic variables; $r_c=R$ (characteristic length scale in the r-coordinate) and $z_c=b$ (characteristic length scale in z-coordinate). It is not immediately obvious how to specify the characteristic pressure (or stress) and velocity. In fact, we shall see that the most appropriate choices for the characteristic pressure and velocity depend upon the condition of the problem. For the moment, we simply denote the characteristic velocity for motion in the radial direction as u_c. By means of the continuity equation, the velocity component w is characterized by $w_c=\varepsilon u_c$. Furthermore, since in the thin-film lubrication flow the dominant viscous force is always balanced by the pressure force, the characteristic scale for the pressure is shown to be related to the characteristic velocity u_c by $p_c=\mu u_c R/b_2$. All that remains for nondimensionalization of the problem is to specify either the characteristic velocity u_c or the characteristic pressure p_c depending upon the condition of the problem. In this section, we consider the inertia contributions for the two specific cases; one in which the pressure drop, ΔP, through the gap is fixed at a constant value ΔP_0 and the other in which the injection rate Q remains unchanged, *i.e.*, $Q=Q_0$ at all times. In the former problem, the obvious choice for the characteristic pressure is $p_c=\Delta P_0$ and thus $u_c=\Delta P_0 b^2/\mu R$ and $w_c=\Delta P_0 b^3/\mu R^2$. On the other hand,

in the latter case, the characteristic velocity u_c is specified by $u_c=Q_0/Rb$ and it follows that $p_c=\mu Q_0/b^3$ and $w_c=Q_0/R^2$.

Let us consider the continuity equation and Navier-Stokes equation in the nondimensionalized form based on the characteristic variables mentioned above:

$$\frac{1}{r}\frac{\partial}{\partial r}(ru)+\frac{\partial w}{\partial z}=0 \tag{2}$$

$$Re\left(u\frac{\partial u}{\partial r}+w\frac{\partial u}{\partial z}\right)=-\frac{\partial P}{\partial r}+\frac{\partial^2 u}{\partial z^2}+O(\varepsilon^2) \tag{3}$$

$$\varepsilon^2 Re\left(u\frac{\partial w}{\partial r}+w\frac{\partial w}{\partial z}\right)= -\frac{\partial P}{\partial z}+\varepsilon^4\frac{1}{r}\frac{\partial}{\partial r}\left(r\frac{\partial w}{\partial r}\right)+\varepsilon^2\frac{\partial^2 w}{\partial z^2} \tag{4}$$

Here, the Reynolds number Re is defined by

$$Re=\frac{\rho u_c b^2}{\mu R} \tag{5}$$

which is very small (*i.e.*, $Re\ll 1$) in the thin-film lubrication limit, $\varepsilon\ll 1$. The boundary conditions to be satisfied are no-slip condition on the surface of each disk, *i.e.*,

$$\vec{u}=0 \text{ at } z=\pm 1 \tag{6}$$

It is noteworthy that the solution for the velocity field $\vec{u}$ cannot, however, be forced to satisfy any boundary conditions at the inlet and outlet edges (*i.e.*, $r=\kappa$ and 1, respectively) without over-specifying $\vec{u}$. Since the thin-film lubrication approximation neglects the second-order derivative terms with respect to r, which are $O(\varepsilon^2)$, in the equation of motion, a solution of leading order in ε no longer requires boundary conditions at both $r=\kappa$ and $r=1$. Instead, we require only that the thin-film solution match with the solutions in the regions outside the thin-film [9, 10], and this matching condition does not influence the form of the leading order solution in the thin-film region which we intend to determine in the present paper.

2. Asymptotic Solutions

Let us then consider the small but nonzero inertial effects in which the governing equations and boundary conditions are (2)-(4) and (6). The case of $Re=0$ is just the normal lubrication problem for parallel surfaces without inertia. For small but nonzero value of Re, on the other hand, we simply expect a solution in the form of a regular perturbation expansion in Re, *i.e.*,

$$\vec{u}=\vec{u}_0+Re\vec{u}_1+\cdots \tag{7}$$

$$P=P_0+ReP_1+\cdots \tag{8}$$

in which the subscript i $(=0, 1)$ denotes the level of approximation.

The governing equations at each order can be obtained by substituting the expansions (7) and (8) into the governing Eqs. (2)-(4) and boundary condition (6) and collecting terms of equal order in Re. Then, the governing equation for the $O(1)$ problem is simply given by

$$\frac{\partial P_0}{\partial r}=\frac{\partial^2 u_0}{\partial z^2} \tag{9}$$

with the boundary condition to be satisfied

$$u_0=0 \text{ at } z=\pm 1 \tag{10}$$

By noting that P_0 is a function of r and independent of z in the limit of $\varepsilon\to 0$, the $O(1)$ solution can be obtained by integrating (9) in terms of z and then applying boundary condition (10):

$$u_0=\frac{1}{2}\left(\frac{\partial P_0}{\partial r}\right)(z^2-1) \tag{11}$$

The unknown pressure gradient $(\partial P_0/\partial r)$ can be determined from the fact that the volume flow rate Q_0 is independent of r and constant.

$$Q_0=2\pi r\int_{-1}^{+1}u_0 dz=-\frac{4\pi r}{3}\frac{\partial P_0}{\partial r} \tag{12}$$

It thus follow that the pressure distribution is given by

$$P_0=-\frac{3}{4\pi}Q_0\ln r \tag{13}$$

in which, for convenience, we take the pressure at the outer edge of the disk as a reference pressure *i.e.*, $P(r=1)=P_{ref}=0$. As pointed out by Bird et al. [3] the pressure distribution decreases logarithmically downstream in the absence of the fluid inertia. Combining (12) and (13), the injection flow rate without fluid inertia can be related to the pressure drop $\Delta P_0[\equiv P_0^{in}-P_0^{out}>0$, where $P_0^{in}=P_0(r=\kappa)$ and $P_0^{out}=P_0(r=1)]$ through the gap:

$$Q_0=-\frac{4\pi\Delta P_0}{3\ln\kappa} \text{ and } \frac{\partial P_0}{\partial r}=\frac{\Delta P_0}{\ln\kappa}\frac{1}{r} \tag{14}$$

Then, the $O(1)$ solution for the velocity distribution $\vec{u}_0=(u_0, 0, w_0)$ is completed as:

$$u_0=\frac{1}{2}\frac{\Delta P_0}{\ln\kappa}\frac{1}{r}(z^2-1) \text{ and } w_0=0 \tag{15}$$

It can be noted that the velocity distribution is radial and has a parabolic profile. The magnitude of the radial velocity decreases like r^{-1}. This is identical to the result of Bird et al. in the limit $Re \to 0$.

We can predict inertia effects in the radial flow between two parallel disks by considering $O(Re)$ solution, which should satisfy

$$\frac{1}{r}\frac{\partial}{\partial r}(ru_1)+\frac{\partial w_1}{\partial r}=0 \tag{16}$$

$$u_0\frac{\partial u_0}{\partial r}=-\frac{\partial P_1}{\partial r}+\frac{\partial^2 u_1}{\partial z^2} \tag{17}$$

P_1 is also a function of r only due to the thin-film approximation. Using the $O(1)$ solution given by (15), the differential Eq. (17) can be solved by satisfying the boundary condition, $u_1=0$ at $z=\pm 1$. The solution for the $O(Re)$ radial velocity is

$$u_1=\frac{1}{2}\left(\frac{\partial P_1}{\partial r}\right)(z^2-1)\\ \frac{(z^2-1)}{120r^3}\left(\frac{\Delta P_0}{\ln\kappa}\right)^2(z^4-4z^2+11) \tag{18}$$

The unknown inertia correction to the pressure gradient $\partial P_1/\partial r$ depends on the condition of the problem. As we mentioned earlier, we consider, in this section, two distinct cases; in the first case, the pressure difference between inlet and outlet of the gap is fixed (equivalently, the inlet pressure is maintained constant) and, in the second case, the injection flow rate through the gap remains constant.

We begin with the first case for the fixed pressure drop. In this case, the inertia contribution to the pressure gradient can be determined from the fact that the inertia correction to the injection flow rate is always independent of r as a consequence of the overall material balance, *i.e.*,

$$\frac{\partial Q_1}{\partial r}=\frac{\partial}{\partial r}\int_{-1}^{+1}2\pi r u_1 dz=0 \tag{19}$$

By substituting u_1 of (18) into (19), we get

$$\frac{\partial P_1}{\partial r}=\frac{6}{35r^3}\left(\frac{\Delta P_0}{\ln\kappa}\right)^2+\frac{C_1}{r},\ C_1:\text{constant} \tag{20}$$

Now, we can determine the inertia correction to the pressure distribution, P_1, by applying the boundary condition $P_1=0$ at $r=\kappa$ and 1, which is a consequence of the condition of a fixed pressure drop:

$$P_1=\frac{3}{35}\left(\frac{\Delta P_0}{\ln\kappa}\right)^2\left[1-\frac{1}{r^2}+\frac{2-\kappa^2}{\kappa^2}\frac{\ln r}{\ln\kappa}\right] \tag{21}$$

Then, upon substituting (21) into (18), the inertia correction to the radial velocity, u_1, is readily evaluated as:

$$u_1=\left(\frac{\Delta P_0}{\ln\kappa}\right)^2\frac{(z^2-1)}{r}\left(\frac{3}{70}\frac{(1-\kappa^2)}{\kappa^2\ln\kappa}-\frac{7z^4-28z^2+5}{840r^2}\right) \tag{22}$$

In view of the continuity Eq. (16), the nonzero vertical component of the velocity w_1 is given by

$$w_1=-\frac{1}{r^4}\left(\frac{\Delta P_0}{\ln\kappa}\right)^2\frac{z(z^2-1)^2(z^2-5)}{420} \tag{23}$$

which is entirely due to the fluid inertia.

The inertia correction to the injection flow rate can be determined from the known solution for the $O(Re)$ radial velocity u_1 of (22). The result is

$$Q_1=-\frac{4\pi}{35}\frac{(\Delta P_0)^2}{(\ln\kappa)^3}\frac{(1-\kappa^2)}{\kappa^2} \tag{24}$$

which is always positive for $0<\kappa<1$. Thus, the inertia of the intervening fluid increases the injection rate. This is a consequence of the fact that in this flow configuration the fluid is actually decelerating like r^{-1} as it travels downstream. But, the effect of inertia is to inhibit (or slow) the rate of deceleration, and the fluid velocity in the radial direction actually moves faster than it does without any inertia present. In Figure 3, the inertia correction to the injection flow rate Q_1 is plotted as a function of the geometric parameter κ. Given a fixed pressure drop ΔP_0, the magnitude of the pressure gradient increases monotonically with κ, as noted from (14), and so does the injection flow rate Q_0 in the absence of the fluid inertia. However, it can be seen that the inertia contribution Q_1 exhibit a minimum at about $\kappa=0.25$. This peculiar result is due to the fact that the convective inertia, $u_0(\partial u_0/\partial r)$, in the equation of motion becomes very large in both the asymptotic limits $\kappa \to 0$ and $\kappa \to 1$:

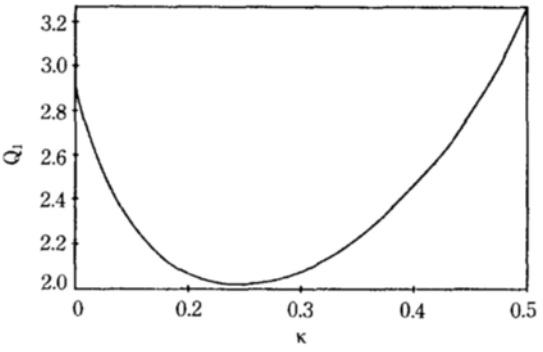

Fig. 3. Inertia contribution to the injection flow rate as a function of the geometric parameter κ for $\Delta P_0=1$.

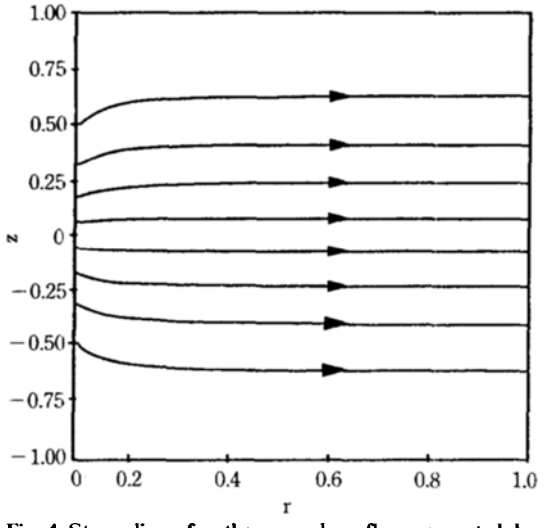

Fig. 4. Streamlines for the secondary flow generated by fluid inertia in the radial source flow under the condition of a fixed pressure drop.

$$u_0\frac{\partial u_0}{\partial r} \sim \begin{cases} \dfrac{1}{\kappa^3(\ln\kappa)^2} & \text{as } \kappa\to 0 \\ \dfrac{1}{(\ln\kappa)^2} & \text{as } \kappa\to 1 \end{cases}$$

For the case of a constant pressure drop, the stream function for the secondary flow induced by fluid inertia is given as

$$\Psi_1 = -\frac{1}{70}\frac{(\Delta P_0)^2}{(\ln\kappa)^3}\frac{(1-\kappa^2)}{\kappa^2}(z^3-3z) + \left(\frac{\Delta P_0}{\ln\kappa}\right)^2\frac{z(z^2-1)^2(z^2-5)}{840r^2} \tag{25}$$

In Figure 4, the streamlines for the inertia-induced secondary flow are plotted for $\kappa=0.1$ and $\Delta P_0=1$. As shown in the figure, the streamlines near $r\approx\kappa$ are not parallel to the disk and similar to those generated by a mass source located at the origin in the two parallel disks.

Finally, let us turn to the second case of a constant injection flow rate (*i.e.*, $Q=Q_0$). It is obvious that the leading-order solution, (14) and (15), does not change and remains valid. All that changes is inertia correction for the pressure distribution $\partial P_1/\partial r$ in (18), which depends on the condition for the problem. Since the injection flow rate Q is unchanged and remains constant, $Q=Q_0$, the inertia correction should satisfy the constraint,

$$Q_1 = \int_{-1}^{+1} 2\pi r u_1 dz = 0 \tag{26}$$

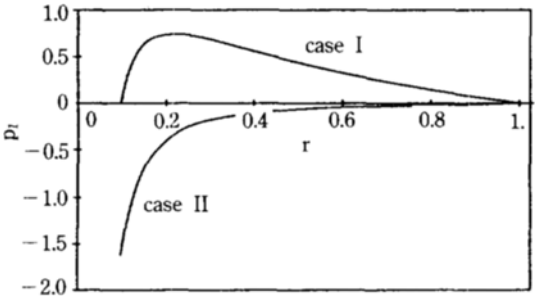

Fig. 5. Inertia correction to the pressure distribution as a function of r for $\kappa=0.1$ and $\Delta P_0=1$: case I, for a fixed pressure drop; case II, for a fixed injection rate.

It thus follows from (18) that

$$\frac{\partial P_1}{\partial r} = \frac{6}{35}\frac{1}{r^3}\left(\frac{\Delta P_0}{\ln\kappa}\right)^2 \text{ and } P_1 = \frac{3}{35}\left(\frac{\Delta P_0}{\ln\kappa}\right)^2\left(1-\frac{1}{r^2}\right) \tag{27}$$

In Figure 5, the inertia correction to the pressure distribution is plotted as a function of r for $\kappa=0.1$ and $\Delta P_0=1$. Also included for comparison is the inertia contribution to the pressure for the preceding case of a fixed pressure drop. It can be easily seen from the figure that the inertia correction is negative everywhere in the present case of a fixed injection flow rate, and the pressure gradient associated with the inertia-induced secondary flow is positive, which is a source of reverse flow, as we shall see shortly. On the other hand, in the foregoing case of a fixed pressure drop the inertia contribution to the pressure is positive everywhere and possesses a maximum $r=\sqrt{2\kappa^2\ln\kappa/\kappa^2-1}$. Further, the positive pressure gradient near $r=\kappa$ associated with fluid inertia causes the secondary flow to exhibit the non-parallel streamlines near the inlet region, and the positive pressure gradient downstream results in the positive correction to the injection flow rate with no recirculating flow, as are seen in Figure 3 and 4. It is worth pointing out that since the inertia correction to the inlet pressure is negative under the condition of a fixed flow rate, the overall pressure drop is smaller than it would be without any inertia present. Thus, in the presence of the fluid inertia, the same flow rate can be achieved with less power consumption.

The inertia contribution to the velocity distribution can be easily determined from (18) and the continuity Eq. (16) :

$$u_1 = -\left(\frac{\Delta P_0}{\ln\kappa}\right)^2\frac{1}{r^3}\frac{(z^2-1)(7z^4-28z^2+5)}{840} \tag{28}$$

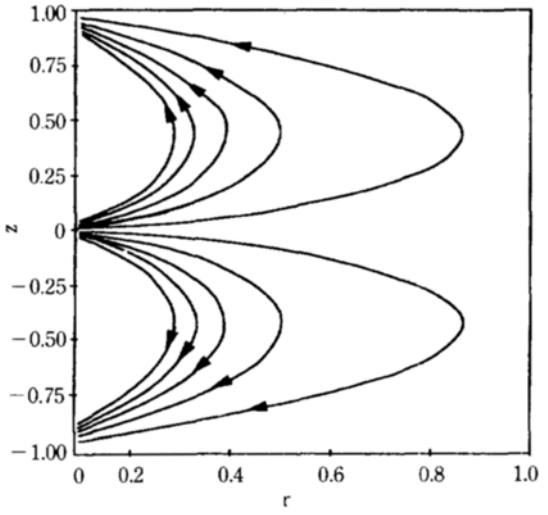

Fig. 6. Streamlines for the secondary flow generated by fluid inertia in the radial source flow under the condition of a fixed injection rate.

$$w_1=-\left(\frac{\Delta P_0}{\ln\kappa}\right)^2\frac{1}{r^4}\frac{z(z^2-1)^2(z^2-5)}{420} \tag{29}$$

It is noteworthy that although the radial component u_1 is different from the previous result, the z-component w_1 is the same as in the previous case. Finally, the stream function of the inertia-induced secondary flow for the case of a constant flow rate can be determined as follows:

$$\Psi_1=\frac{1}{r^2}\left(\frac{\Delta P_0}{\ln\kappa}\right)^2\frac{z(z^2-1)^2(z^2-5)}{840} \tag{30}$$

In Figure 6, the streamlines of the secondary flow induced by fluid inertia are plotted for $\kappa=0.1$ and $\Delta P_0=1$. It can be noted from Figures 4 and 6 that the secondary flow pattern for the case of a fixed flow rate is quite different from that for the preceding case of a fixed pressure drop. The secondary flow with a fixed injection rate exhibits recirculating streamlines, which is qualitatively similar to the numerical result [1]. As noted earlier, reverse flow is caused primarily by the positive value of inertia corrections to the pressure gradient, $\partial P_1/\partial r$ in (27).

FLOW BETWEEN TWO COAXIALLY ROTATING DISKS

1. Formation of Problem

Let us first consider the governing equations and the boundary conditions for the flow between two coaxially rotating disks, as shown in Figure 2. As in the preceding examples in section 2, we take a cylindrical coordinate system (r, θ, z), in which the disks occupy the planes $z=0$ and $z=H$ and are coaxially rotating with angular velocities Ω_1 and Ω_2, respectively.

In view of the axisymmetry of the problem, the continuity equation and the Navier-Stokes equation for the velocity distribution $\vec{u}=(u, v, w)$ in (r, θ, z) can be expressed as:

$$\frac{1}{r}\frac{\partial}{\partial r}(ru)+\frac{\partial w}{\partial z}=0 \tag{31}$$

$$Re\left(u\frac{\partial u}{\partial r}+w\frac{\partial u}{\partial z}-\frac{v^2}{r}\right)=-\frac{\partial P}{\partial r}+\frac{\partial^2 u}{\partial z^2}+O(\varepsilon^2) \tag{32}$$

$$Re\left(u\frac{\partial v}{\partial r}+\frac{uv}{r}+w\frac{\partial v}{\partial z}\right)=\frac{\partial^2 v}{\partial z^2}+O(\varepsilon^2) \tag{33}$$

in which the variables are nondimensionalized with respect to the characteristic variables: $r_c=R$, $z_c=H$, $u_c=v_c=\Omega_2 R$, $w_c=\Omega_2 H$, *and* $p_c=\mu R^2\Omega_2/H^2$. The Reynolds number in this problem is thus defined by $Re=\rho\Omega_2 H^2/\mu$ which is very small but finite in the thin-film limit, $\varepsilon\to 0$. In addition, from the equation of motion in the z-direction and the axisymmetry of the problem, it can be easily shown that

$$\frac{\partial P}{\partial\theta}=0 \text{ and } \frac{\partial P}{\partial z}=O(\varepsilon^2) \tag{34}$$

and thus the pressure distribution may be considered to be a function of r only in the thin-film limit.

The boundary conditions which must be satisfied by the solutions to the governing equations are as follows:

$$u=w=0,\ v=\beta r \text{ at } z=0 \tag{35}$$

$$u=w=0,\ v=r \text{ at } z=1 \tag{36}$$

We have now three equations relating the four unknown functions u, v, w and P, together with the boundary conditions (35) and (36), which contain two dimensionless parameters, Re and $\beta=\Omega_1/\Omega_2$. Thus, in order to determine the unique solution to the problem, we need one more equation supplemented to (31)-(33). This is the overall mass balance which can be written as

$$\int_0^1 2\pi r u dz=0 \tag{37}$$

2. Asymptotic Solution

Following the preceding analysis in section 2, we can determine the solution to this problem as an asymptotic series, (7) and (8). The governing equations for

the leading-order terms, $\vec{u}_0$, P_0 in (7) and (8), can be obtained by simply taking the limit $Re \to 0$ in the governing equations and the boundary conditions, (31)-(37). The solution of the leading order problem is straightforward and simply given as:

$$u_0 = w_0 = 0 \text{ and } v_0 = (1-\beta)rz + \beta r \tag{38}$$

$$P_0 = 0 \tag{39}$$

which is identical to the result of the rheometry flow between two coaxially rotating disks without any inertia present [5].

The governing equations for the first inertia corrections can be obtained as:

$$\frac{1}{r}\frac{\partial}{\partial r}(ru_1) + \frac{\partial w_1}{\partial z} = 0 \tag{40}$$

$$-\frac{v_0^2}{r} = \frac{\partial^2 u_1}{\partial z^2} - \frac{\partial P_1}{\partial r} \tag{41}$$

$$\frac{\partial^2 v_1}{\partial z^2} = 0 \tag{42}$$

with the boundary conditions

$$u_1 = v_1 = w_1 = 0 \text{ at } z = 0 \tag{43}$$

$$u_1 = v_1 = w_1 = 0 \text{ at } z = 1 \tag{44}$$

together with the overall mass balance

$$\int_0^1 2\pi r u_1 dz = 0 \tag{45}$$

After some algebra, the first inertia contribution to the velocity and pressure distributions can be expressed as follows:

$$u_1 = -\frac{rz(z-1)}{60}[5(1-\beta)^2 z^2 + 5(3\beta+1)(1-\beta)z - (6\beta+4)(1-\beta)] \tag{46}$$

$$v_1 = 0 \tag{47}$$

$$w_1 = \frac{z^2(z-1)^2}{30}[(1-\beta)^2 z + (1-\beta)(3\beta+2)] \tag{48}$$

$$P_1 = \frac{r^2}{20}[3(1-\beta)^2 + 10\beta] \tag{49}$$

From the velocity distribution induced by fluid inertia, the stream function of the secondary flow can be obtained as

$$\Psi_1 = \frac{r^2 z^2 (z-1)^2}{60}[(1-\beta)^2 z + (1-\beta)(3\beta+2)] \tag{50}$$

In Figure 7 and 8, the streamlines of the secondary flow are plotted for $\beta = 1/2$ and $\beta = -1$, respectively.

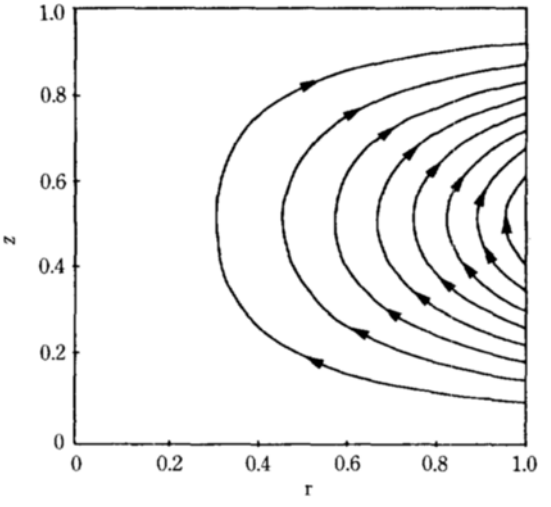

Fig. 7. Streamlines of the secondary flow generated by fluid inertia in the flow between coaxially rotating disks for the parameter $\beta = 1/2$.

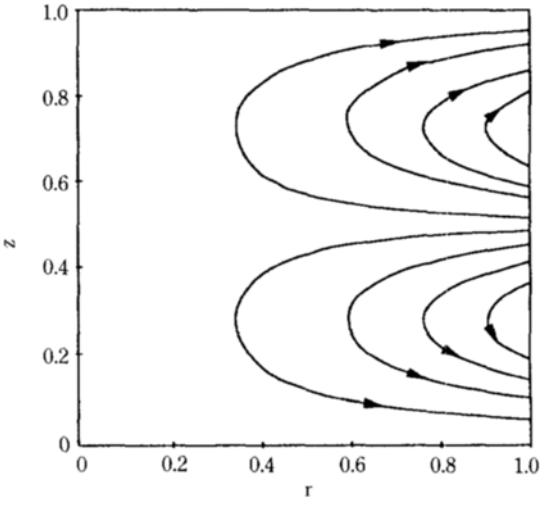

Fig. 8. Streamlines of the secondary flow generated by fluid inertia in the flow between coaxially rotating disks for the parameter $\beta = -1$.

It can be noted that the secondary flow pattern depends on the single parameter β and can be classified into three distinct families. When $-2/3 < \beta < 1$, the radial velocity will be inward near the bottom plate and outward near the top plate since the dominant centrifugal force near the top plate swamps that generated by the bottom plate. On the other hand, when $\beta < -3/2$ or $\beta > 1$, which is the counterpart of the previous case of $-2/3 < \beta < 1$, the bottom plate acts as a centrifugal

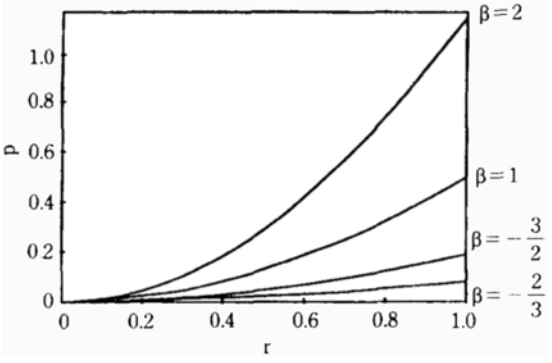

Fig. 9. Inertia-induced pressure distribution in the flow between coaxially rotating disks.

fan and the secondary flow is in the opposite direction. When $-3/2<\beta<-2/3$, the centrifugal forces in the vicinity of the rotating plates are competitive each other and there is a plane between the gap on which the azimuthal component of the velocity vanishes. Thus the radial flow in the neighborhood of each disk will be outward.

The inertia contribution to the pressure distribution, given by (49), is due solely to the fluid inertia (so that $P_1=0$ in the absence of the fluid inertia). As shown in Figure 9, the inertia-induced pressure distribution increases quadratically in r, and the resulting positive pressure gradient creates the recirculating secondary flow. It can be also seen that the inertia induced pressure possesses a minimum value at $\beta=-2/3$.

One of the quantities of potential significance to be determined is the inertia correction to the hydrodynamic torque acting on each disk to sustain the prescribed rotational motion. To do this, however, we must continue for one more step in the solution precedure in the expansions (7) and (8) since the first inertia correction to the azimuthal velocity component v_1 is zero and thus the corresponding correction to the torque vanishes.

The second order solution can also be determined from the following governing equations

$$\frac{1}{r}\frac{\partial}{\partial r}(ru_2)+\frac{\partial w_2}{\partial z}=0 \tag{51}$$

$$\frac{\partial^2 u_2}{\partial z^2}=\frac{\partial P_2}{\partial r} \tag{52}$$

$$u_1\frac{\partial v_0}{\partial r}+\frac{u_1 v_0}{r}+w_1\frac{\partial v_0}{\partial z}=\frac{\partial^2 v_2}{\partial z^2} \tag{53}$$

with the same forms of boundary conditions and overall material balance as (43)-(45). The solution for the $O(Re^2)$ problem can be shown straightforwardly to be:

$$u_2=w_2=0 \tag{54}$$

$$\begin{aligned} v_2=&-\frac{r(1-\beta)z(z-1)}{6300}[20(1-\beta)^2z^5\\ &+20(6\beta+1)(1-\beta)z^4\\ &+(237\beta^2+16\beta-43)z^3-(183\beta^2+124\beta+8)z^2\\ &+(27\beta^2+16\beta-8)z+(27\beta^2+16\beta-8)] \end{aligned} \tag{55}$$

$$P_2=0 \tag{56}$$

Thus, the inertia-induced flow at $O(Re^2)$ is purely azimuthal and has no contribution to the pressure distribution.

Finally, the hydrodynamic torques on the upper and lower disks can be easily calculated from the completed solution $v=v_0+Re^2v_2$ given by (38) and (55) and are as follows

$$T_{upper}=\frac{(1-\beta)}{3}\left[1+Re^2\left(\frac{27+16\beta-8\beta^2}{6300}\right)\right] \tag{57}$$

$$T_{lower}=\frac{(1-\beta)}{3}\left[1+Re^2\left(\frac{27\beta^2+16\beta-8}{6300}\right)\right] \tag{58}$$

As noted, the inertia contribution to the hydrodynamic torque appears at $O(Re^2)$. Thus, the torque required to sustain the angular motion is no longer a linear function of the angular velocity. Further, the hydrodynamic torque on each disk is not the same owing to the inertia effects.

CONCLUSION

Convective inertia effects in the motion of fluid layer between two parallel concentric circular plates have been studied using the standard method of asymptotic expansions. This analysis has led to the following conclusions:

(1) Since the fluid is decelerating as it travels downstream in the radial source flow between two parallel disks, the fluid inertia increases the flow rate through the gap under the condition of a fixed pressure drop. The secondary flow pattern with a fixed flow rate exhibiting recirculating streamlines is quite different from that for the case of a fixed pressure drop, in which the secondary flow streamlines are nearly parallel to the primary flow.

(2) In the flow between two coaxially rotating disks the secondary flow pattern depends on the single parameter β which is the ratio of the angular velocities of the two coaxial disks. The unique parameter β classifies the solution into three distinct families. The iner-

tia contribution to the hydrodynamic torque appears at $O(Re^2)$. Because of the inertia effect, the hydrodynamic torques on the top and the bottom disks are not the same.

REFERENCES

1. Raals, J. D.: *J. Fluid Mech.*, **85**, 401 (1978).
2. Allen, D. N. DE G. and Southwell, R. V.: *Quart. J. Mech. Appl. Math.*, **8**, 129 (1955).
3. Bird, R. B., Stewart, W. E. and Lightfoot, E. N.: Transport Phenomena, Wiley & Sons, New York (1960).
4. Karman, T. V.: *Zeits. f. angew. Math. u. Mech.*, **1**, 244 (1921).
5. Tanner, R. I.: Engineering Rheology, Clarendon Press, Oxford (1985).
6. Tichy, J. A. and Winer, W. O.: *Trans. A.S.M.E.* F: *J. Lub. Tech.*, **92**, 588 (1970).
7. Christensen, H.: *Proc. R. Soc. Lond.*, **A226**, 312 (1962).
8. Rohde, S. M., Whicker, D. and Browne, A. L.: *Trans. A.S.M.E.* F: *J. Lub. Tech.*, **98**, 401 (1978).
9. Yang, S.-M. and Leal, L. G.: *Int. J. Heat & Flow*, to appear (1992).
10. Hamza, E. A. and MacDonald, D. A.: *J. Fluid Mech.*, **109**, 147 (1981).
11. Weinbaum, S., Lawrence, C. J. and Kuang, Y.: *J. Fluid Mech.*, **156**, 463 (1985).